NATIONAL AERONAUTICS AND SPACE ADMINISTRATION

EARTH RESOURCES SURVEY PROGRAM

TECHNICAL LETTER NASA-35

EVALUATION OF NIMBUS I HIGH RESOLUTION INFRARED RADIOMETER (HRIR) IMAGERY

By

M. A. Conti
U. S. Geological Survey
Washington, D. C.

April, 1967

Prepared by the Geological Survey for the
National Aeronautics and Space Administration (NASA)
under NASA Contract No. R-09-020-111

MANNED SPACECRAFT CENTER
HOUSTON, TEXAS

UNITED STATES
DEPARTMENT OF THE INTERIOR
GEOLOGICAL SURVEY
WASHINGTON, D.C. 20242

Technical Letter
NASA - 35
April 1967

Dr. Peter C. Badgley
Program Chief,
Earth Resources Survey
Code SAR - NASA Headquarters
Washington, D. C. 20546

Dear Peter:

Transmitted herewith is one copy of:

TECHNICAL LETTER NASA-35

EVALUATION OF NIMBUS I HIGH RESOLUTION INFRARED

RADIOMETER (HRIR) IMAGERY*

by

M. A. Conti**

Sincerely yours,

William A. Fischer
Research Coordinator
Earth Orbiter Program

*Work performed under NASA Contract No. R-09-020-011
**U.S. Geological Survey, Washington, D. C.

UNITED STATES
DEPARTMENT OF THE INTERIOR
GEOLOGICAL SURVEY

TECHNICAL LETTER NASA-35

EVALUATION OF NIMBUS I HIGH RESOLUTION INFRARED RADIOMETER (HRIR) IMAGERY*

by

M. A. Conti**

April 1967

These data are preliminary and should not be quoted without permission

Prepared by the Geological Survey for the National Aeronautics and Space Administration (NASA)

*Work performed under NASA Contract No. R-09-020-011
**U.S. Geological Survey, Washington, D. C.

CONTENTS

ILLUSTRATIONS

EVALUATION OF NIMBUS I HIGH RESOLUTION INFRARED RADIOMETER (HRIR) IMAGERY

by

M. A. Conti

ABSTRACT

Geologic features imaged by the HRIR instrument aboard the Nimbus satellite include volcanic and thermal zones, terrain-thermal reversals, thermal soil patterns, and polar ice features. Poor resolution, small scale, and other factors, however, severely limit the quality of the imagery and the detectability of geologic features on a worldwide scale. Furthermore, as the imagery is inadequate for certain specialized geologic studies, such as lithologic discriminations, it is not suitable for most mapping purposes. Experience with Nimbus imagery, however, provides a means for development of criteria for future instrumentation and interpretation procedures for geologic investigations.

INTRODUCTION

The Nimbus infrared radiometer detects emitted and reflected infrared radiation from the surface of any body viewed that is more or less opaque to radiation within the wavelength interval detected, whether a landmass, water, or a cloud. The relation of actual surface temperatures to blackbody-equivalent temperatures recorded by the radiometer depends upon the emissivity of the surface imaged. Radiant energy emitted at a given temperature may differ according to nature of materials (rock versus soil), condition of solid surface (rough versus polished), and other factors, and may therefore result in apparent but not real thermal contrasts. However, certain factors affecting radiation recorded by the scanner, particularly temperature differences due to altitude and thermal properties of the terrestrial surface such as heat capacity and thermal diffusivity, appear to overshadow emissivity differences in the Nimbus record. These have been indicated by numerous ground and ocean surface temperature checks and atmospheric lapse-rate (vertical temperature change) estimates as well as by obvious prominence of major water, cloud, and relief features in the imagery (Nordberg, 1965) (figures 1 and 2; for annotations see caption list). For convenience in this report, sources of higher radiant energy (which appear darker on the Nimbus images) will be referred to as "warm" and sources of lower radiant energy (lighter tones), as "cold", in conformity with common usage in the field.

IMAGERY OF GEOLOGIC FEATURES

In addition to meteorologic and oceanographic features, discussion of which is not within the scope of this report, certain geologic, topographic, glacial, hydrologic, pedologic, and volcanic features also were imaged from Nimbus I. Geologic features that can be identified in the almost exclusively nocturnal Nimbus infrared imagery include:

1. Continents and islands in contrast to warmer seas and oceans.
2. Icecaps and ice shelves as well as sea ice, in contrast to warmer land and oceans.
3. Mountain ranges in contrast to warmer lowlands.

On a more localized basis, a number of additional features have been distinguished in the imagery:

4. Volcanic craters and possible thermal zones.
5. Terrain-thermal reversals, warmer slopes surrounding a cooler desert basin or flanking mountains.
6. Large lakes, nocturnally warmer than surroundings.
7. Very deep distinctive valleys which often are warmer because of lower elevation than surrounding uplands.
8. Distinction among cold continental icecaps, warmer permanent ice shelves, and still warmer seasonal sea ice, as well as recognition of openings, areas of ice breakups, and major cracks in ice.
9. Narrow stream courses and flanking moist zones in desert environments.
10. Fine thermal patterns in desert soils.

Some of the features cited, particularly numbers 1-3, 6 and 7, can be viewed more successfully in the Advanced Vidicon Camera System (AVCS) visible - light spectrum imagery and therefore need not be further treated. The gross infrared contrasts between these major continental and oceanic features are readily apparent in striking examples from Africa and the Near East (figures 1 and 2). The other features (4,5,8-10) involve aspects not normally or adequately imaged by the Nimbus AVCS imagery.

The volcanic craters Mauna Loa and Kilauea are identifiable as tiny hot spots in a magnified image of Hawaii although Mauna Kea does not form a hot spot (figure 3; also Gawarecki, Lyon, and Nordberg, 1965). Such features are often too small to identify in the AVCS imagery and in this respect the HRIR imagery can be superior. Thermal zonation is also evident in figure 3, and appears to correspond primarily to elevation differences on the island (figure 4). Comparison of the magnified Nimbus infrared imagery of Kilauea (figure 3) with that of a low-altitude infrared aerial survey (figure 5; also Fischer, Moxham, and others, 1964) shows the loss of thermal detail in the former resulting from both the elevation difference and the poorer spatial and thermal resolution. Nevertheless, the primary zonation of central hot spot and cold collar is surprisingly distinct in the Nimbus image. Inasmuch as the crater is somewhat smaller than even the minimal HRIR resolution unit at subpoint perigee, this example indicates that subresolutional features may show up if they contrast sharply in temperature with their surroundings. Yet, despite volcanic pinpointing in Hawaii, no hot spots have been recognized corresponding

to the dormant volcanoes with fumarolic activity near the Atacama Desert in South America, possibly because of less thermal contrast, spurious signal interference, small scale of the volcanic features, or meteorologic interference.

Dark bands at the Salar de Atacama, within a basin in the Atacama Desert, Chile and at the Sierra del Pié de Palo in Argentina are thought by Nordberg (1965) to relate to differences in thermal properties of the materials at the basin bottom and on the flanking slopes, resulting in higher slope temperatures at night despite the higher elevation (figures 6 and 7). However, Gawarecki, Lyon, and Nordberg (1965) point out the possible role of emissivity differences (differences in energy emitted by sources at the same temperature), atmospheric temperature inversions, and thermal springs in these situations. Emissivity factors may overshadow temperature differences in the inner band haloing the Salar de Atacama itself, reflecting pronounced differences in soil salinity. But the possible role of moisture differences cannot be eliminated in this instance, although the salar is normally not wet or inundated. In any case, the features represented by the halos, whatever their actual nature and cause, are not evident in the Nimbus AVCS imagery.

The continental icecap is distinguishable from warmer shelf and sea ice in the Ross Sea area, and farther east in Antarctica the ice shelf and sea ice themselves are distinguishable (Nordberg, 1965; also Gawarecki, Lyon, and Nordberg, 1965). The thermal differences may relate to thickness of ice and warming influence of the ocean as well as elevation differences. Breakups in the ice, cracks, and open areas, of course, yield higher thermal readings due to the exposure of warmer ocean waters, and detail corresponding to such features may show up better by thermal patterns in infrared imagery than by visible patterns in the AVCS imagery (figure 8). The lack of imagery of the North Pole precludes an examination of the thin ice in that region.

Many streams less than 1 km wide flowing in desert areas stand out prominently in the Nimbus HRIR imagery, though well below the maximum resolution limit of the instrument at subpoint perigee and often below the resolution limit even of the AVCS imagery (Nordberg, 1965). Among such streams recognizable are the Río Zanjón and the Río Bermejo east of the Sierra del Pié de Palo, Argentina (figure 6). Since these two rivers are less than a few hundred meters wide, usually dry, and unentrenched, the radiometer has probably detected the warmer broad moist alluvial belts in which the streams flow, in contrast to the arid, nocturnally cooler desert surroundings. On the other hand, only vague indications can be found of the great Amazon River, due to the lack of climatic and moisture (therefore thermal) contrasts.

Fine thermal patterns discernible in the soils of North African and Near Eastern deserts are ascribed by Nordberg (1965) to variations in soil temperatures. The temperature differences may be due to differences in thermal properties, possibly in places modified by moisture variations. More specifically, in the lowlands just north of the Caspian Sea, contrasting zones of lighter and darker image tones are noticeable upon close examina-

tion (figure 1). Comparison with terrain maps of the area discloses that the lighter tones correspond to sand dune belts and the darker tones, to neighboring alluvial areas. Inasmuch as the elevation differences are negligible, the tonal variations are probably related to differences in thermal properties or moisture content, both of which affect heat retention. The relatively small differences in moisture that might be detected as infrared phenomena because of nocturnal differential cooling are not suceptible to AVCS imaging.

Emissivity and spectral (peak wavelength) differences among rock types have been successfully detected in controlled experiments in the laboratory (Gawarecki, Lyon, and Nordberg, 1965; Lyon, 1965; and Lyon and Burns, 1964). But the intergrated emissivity differences involved are too small to be detected in the Nimbus infrared imagery. As pointed out by Nordberg (1965), not even emissivity differences of a fairly high magnitude, such as of rock versus soil, could be clearly identified and established. Furthermore, the radiometer with its narrow single rather than multiple or broad-spectrum bandpass was not designed to make spectral distinctions adequate for lithologic discriminations. Spectral distinctions permitting graphic "signaturing" of emissivity may be essential for such discriminations, according to some preliminary investigations (Lyon and Burns, 1964; Lyon, 1965), and may permit discrimination of some contrasting rock types, such as those high in silicates versus carbonates (Hovis, 1965).

LIMITATIONS FOR GEOLOGIC USE

Many terrestrial features imaged by the Nimbus radiometer have been imaged locally by airborne radiometers from low altitudes on an experimental basis, often with extremely sharp and detailed results (Fischer, Moxham, and others, 1964). However, the Nimbus I imagery is generally considerably inferior to the low-altitude imagery for a number of reasons. The obvious factors are the extremely small scale and severe planimetric distortion due to east-west image compression near the horizons reflecting the curvature of the earth; east-west image elongation and scale increase below apogee related to increasing velocity and lower altitude of the eccentric orbit; and undulations along the horizons registered subsequent to equatorial crossings, indicative of roll induced by the effect of high-altitude tropical cold clouds on the infrared horizon scanner of the controls system. Other significant disadvantages are:

1. Poor image definition, probably the greatest drawback, due in part to the relatively low spatial resolution of the radiometer (despite its label as a high-resolution instrument), in part to the great altitude (small scale), and in part to the loss of thermal detail in conversion from analog records of 100 signal levels to imagery with only 10 tonal distinctions.

2. Variable temperature corrections required due to differential atmospheric absorption depending upon latitude and scan angle; corrections for spurious signal interference; and limited thermal resolution.

3. Cloud obstruction of many areas and indirect cloud effects such as diffusion of radiation.

4. Dust, haze, and fog effects on radiance, such as scatter, distortion, turbulence, diffraction, and unusual absorption.

5. Lack of a multiple-bandpass or broad-spectrum design for emissivity "signaturing", or continuous emissivity recording.

6. Selection of bandpass for emphasis of cloud features, and lack of adjustment for optimum contrast in terrestrial features.

7. Noise effects (spurious signals), diagonal white lines from periodic noise at 16 cycles per second, separated by constant scan-angle intervals, and east-west bands of alternating dark and light spots from oscillatory noise at 200 cycles per second (Fujita and Bandeen, 1965), the latter a serious interference in image interpretation (figure 3).

8. Gapping of thermal ground data bands below apogee.

GEOLOGIC EVALUATION

Evaluation of the Nimbus I infrared imagery is largely negative for geologic mapping on a wide scale. A possible exception is imagery of drainage and glacial features, which might be of value in correcting the detail of maps of areas lacking conventional airphoto coverage which were clear at night but obstructed by clouds in the daytime and therefore unavailable in the AVCS imagery. The HRIR data could also, for example, contribute temporal data on lake temperatures and for ice temperature contour maps, of possible interest to the hydrologist and glaciologist. But though a variety of geologic, topographic, hydrologic, glacial, pedologic, and a few volcanic features have been detected in some areas, identical features have not been detected or are not apparent in other areas. Even where the features are detected, definition is poor. Lithologic distinctions cannot be made due to the subtlety of emissivity variations among various rock types, the lack of spectral signaturing design of the radiometer, and other factors. Integrated emissivity variations are obscured by differences in thermal properties and total reflectivity of rock types. Effective detection in Nimbus I imagery of features based primarily on emissivity differences would be possible only where specific integrated emissivity differences related to specific materials are particularly great.

RECOMMENDATIONS

It is suggested that limited additional effort, involving some field checks, be directed toward further development of criteria for the detection of features displaying certain thermal patterns, with a view toward application to future improved satellite imagery. Attention should be given to determination of causes of the thermal phenomena observed in the imagery and examination of more imagery of other thermal phenomena, both of Nimbus I and its successor, Nimbus II. The most promising items for study by way of spaceborne infrared radiometer systems are:

1. Ice features in Antarctica and Greenland, especially sea, shelf, and cap ice, and also areas (aside from actual large-scale openings) of thin ice and ice breakup.

2. Terrain-thermal reversals in desert areas, particularly a check of causes, whether due to atmospheric temperature inversions, emissivity differences, differences in thermal properties, or other causes.

3. Soil thermal patterns in deserts, whether due to thermal properties as determined by moisture content or grain size, and the role of emissivity differences.

4. Volcanic regions at high elevations, for a better idea of the extent to which subresolutional crater hot spots can be detected for known active volcanoes. Recent examination of imagery of Nimbus II has lead to detection of another volcanic anomaly - Surtsey volcano, off the south coast of Iceland (Friedman, oral communication, 1967).

5. Conspicuous patterns not yet identified, such as certain lineaments, checked for relationship to topographic, structural geologic, or other features.

6. Thermal fields, such as areas of hot springs, or sites of deep sea volcanic eruptions.

7. Areas of debouchment of hot or cold ground water.

8. Subglacial thermal activity, such as undermining of glaciers or other ice by thermal waters.

9. Extensive areas of uniform lithology or pedology, such as desert hammadas or limestone plateaus, which might be checked for a comparison of emittance properties with those of laboratory samples of the same material.

10. Areas of intensive mineralization, which might be scrutinized to see whether large deposits can be discriminated.

Most of these features may be slow to change or seasonally repetitive if not absolutely constant, so that at least gross aspects and relationships should be observable. Magnification of the image should be increased where it is necessary to make the oscillatory noise pattern more distinguishable from actual radiation patterns. Image improvement by elimination or suppression of this signal is possible electronically by smoothing of the analog curves according to mathematical running means and reimaging, after the method of Fujita and Bandeen (1965). Similarly, there may be some value in producing new images from the tape records at different gain levels in order to bring out more detail in the areas that are now all white or black (provided that the signal was recorded with a sufficiently wide dynamic range) (Gawarecki, oral communication, 1966). Supplementation of the imagery by restoring the greater thermal distinctions of the original analog records on the tapes in the form of digital temperature maps would aid interpretation of some specific features. Although the quality of the imagery could thus be significantly improved, it is doubtful whether such measures would be justifiable for the imagery as a whole, considering the limitations imposed by the poor resolution

and gapped data, and the possibility of finer imagery by successors of Nimbus I, and of Nimbus II as well, in the future. However, such measures could be applied in special instances. In any case, the results of a relatively brief project of this sort should clarify some of the causal relations even though significant features may not be detectable in many areas.

SELECTED REFERENCES

Fischer, W. A., Moxham, R. M., Polcyn, F., and Landis, G. H., 1964, Infrared surveys of Hawaiian volcanoes: Science, v. 146, no. 3645, p. 733-742.

Fujita, T. and Bandeen, W., 1965, Resolution of the Nimbus high resolution infrared radiometer: Jour. of Appl. Meteorol., v. 4, no. 4, p. 492-503.

Gawarecki, S. V., Lyon, R. J. P., and Nordberg, W., 1965, Infrared spectral returns and imagery of the earth from space and their application to geologic problems (in process).

Goldberg, I. L., Foshee, L., Nordberg, W., and Catoe, C., 1965, Nimbus high resolution infrared measurements: Symposium on Remote Sensing of Environments, 3d, Inst. of Sci. and Technol., Univ. of Michigan, 1964, Proceedings, p. 781-788.

Hovis, W. A., Jr., 1965, Infrared sensing of earth surface materials (abs.): Internat. Symposium on Electromagnetic Sensing of the Earth from Satellites.

Lyon, R. J. P., 1965, Analysis of rocks by spectral infrared emission: Econ. Geology, v. 60, no. 4, p. 715-736.

Lyon, R. J. P., and Burns, E. A., 1964, Infrared emittance and reflectance spectra of rough and powdered rock surfaces: Jour. of Geophys. Research (in process).

National Aeronautics and Space Administration, Aeronomy and Meteorology Division, 1965, Nimbus I high resolution radiation data catalog and users' manual: Greenbelt, Goddard Space Flight Center.

National Aeronautics and Space Administration, Scientific and Technical Information Division, 1965, Observations from the Nimbus I meteorological satellite (symposium): Greenbelt, Goddard Space Flight Center.

Nordberg, W., 1965, A review of infrared sensing with meteorological satellites (abs.): Internat. Symposium on Electromagnetic Sensing with Meteorological Satellites.

CAPTION LIST

Figure 1 Nimbus I HRIR image of Caspian Sea region (magnified); A - high clouds, B - low clouds, C - Volga River, D - Caspian lowlands, E - Caspian Sea, F - Aral Sea. Orbit 037, Data Block 13.

Figure 2 Nimbus I HRIR image of southeast Africa (magnified); A - southern highlands of Tanganyika, B - Zanzibar, C - Tanganyika coastal lowlands, D - Lake Nyasa, E - Lake Chilwa, F - Nyasaland ranges, G - Zambesi Valley, H - southeast Rhodesian ranges, J - Basutoland ranges, K - Madagascar, L - Indian Ocean, X - low clouds, Y - high clouds. Orbit 037, Data Block 13.

Figure 3 Nimbus I HRIR image of Hawaiian Islands and vicinity (magnified); A - Mauna Loa, B - Kilauea, C - Mauna Kea. Orbit 250, Data Block 191.

Figure 4 Relief map of Hawaii.

Figure 5 Low-altitude aerial infrared imagery and conventional photography of Kilauea Volcano, Hawaii.

Figure 6 Nimbus I HRIR image of western South America (magnified); A - Atacama Desert, B - Sierra del Pié de Palo. Orbit 246, Data Block 184.

Figure 7 Relief map of Atacama Desert and vicinity, Chile.

Figure 8 Nimbus I HRIR imagery and AVCS imagery, Ross Sea, Antarctica (magnified); Orbit 352, Data Block 317; Orbit 349.

APPENDIX

Evaluation of the photofacsimile imagery derived from radiant energy measurements made by the high resolution infrared radiometer aboard the Nimbus I satellite is enhanced by an understanding of certain technical aspects of the project (National Aeronautics and Space Administration, 1965). The radiometer was designed primarily to provide radiant energy measurements of meteorologic features, such as clouds, convertible to digital temperature maps and photofacsimile radiance imagery. Incident infrared radiation from the earth and clouds was limited by a filter to a bandpass of 3.5-4.2 microns, in the middle infrared spectrum, corresponding to a "window" of minimal atmospheric absorption and attenuation of signal. Almost all of the imagery is nocturnal, eliminating infrared solar reflectance. The instantaneous subpoint field of view of the radiometer varied according to satellite height from about 3.4 x 3.4 km at perigee (423 km) to about 7.3 x 7.3 km at apogee (932 km). These areas represent the ground resolution of the instrument, the smallest areas for which a radiance value (blackbody-equivalent temperature) was recorded on tape in the satellite. The instrument was designed to scan the earth from horizon to horizon (roughly east-west), perpendicularly to the near-polar orbit of the satellite. Thus each scan resulted in a continuous radiometric analog record, equivalent to a running graph, later converted into a narrow band of varying tonal density in the photofacsimile film imagery. The scanning rate was set to make a single sweep during the time it took the satellite to advance southward one resolution distance at apogeal height, and the images are composed of continuous bands of light to dark tone representing thermal patterns, similar in principle to conventional television images. Actually, though the bands retain their width and contiguity and therefore spacing throughout the imagery itself, they represent narrower, gapped bands of thermal ground data for most of the coverage, due to the failure to attain a circular satellite orbit of apogeal radius, for which the scan rate and tape transport had been synchronized. The thermal resolution, the smallest temperature difference detectable by the radiometer, is 1°-2° Kelvin, but the overall thermal correction necessary is as great as 6°-8° in some instances. The subpoint location error is about 16 km at apogee, corresponding to a 1° pointing accuracy for the satellite control system. Each roughly north-south film strip images an area ranging from about 6,500 km in width from horizon to horizon at apogee to about 4,000 km in width at perigee. However, roughly only the central half of this width was sufficiently undistorted to justify addition of gridlines on the images. The scale of the images near subpoint ranges very roughly from 1:30,000,000 at perigee to 1:70,000,000 at apogee, but actually varies considerably with azimuth near perigee due to distortion. Subpoint perigee advanced from lat 20°N. to about lat 80°N. during the 26-day lifetime of the sensory equipment. Of the 368 orbits made by the satellite during those 26 days, readouts of 323 data blocks (continuous strips) were commanded for 194 orbits, providing nearly complete earth coverage, except in the North Polar region, with considerable overlap.

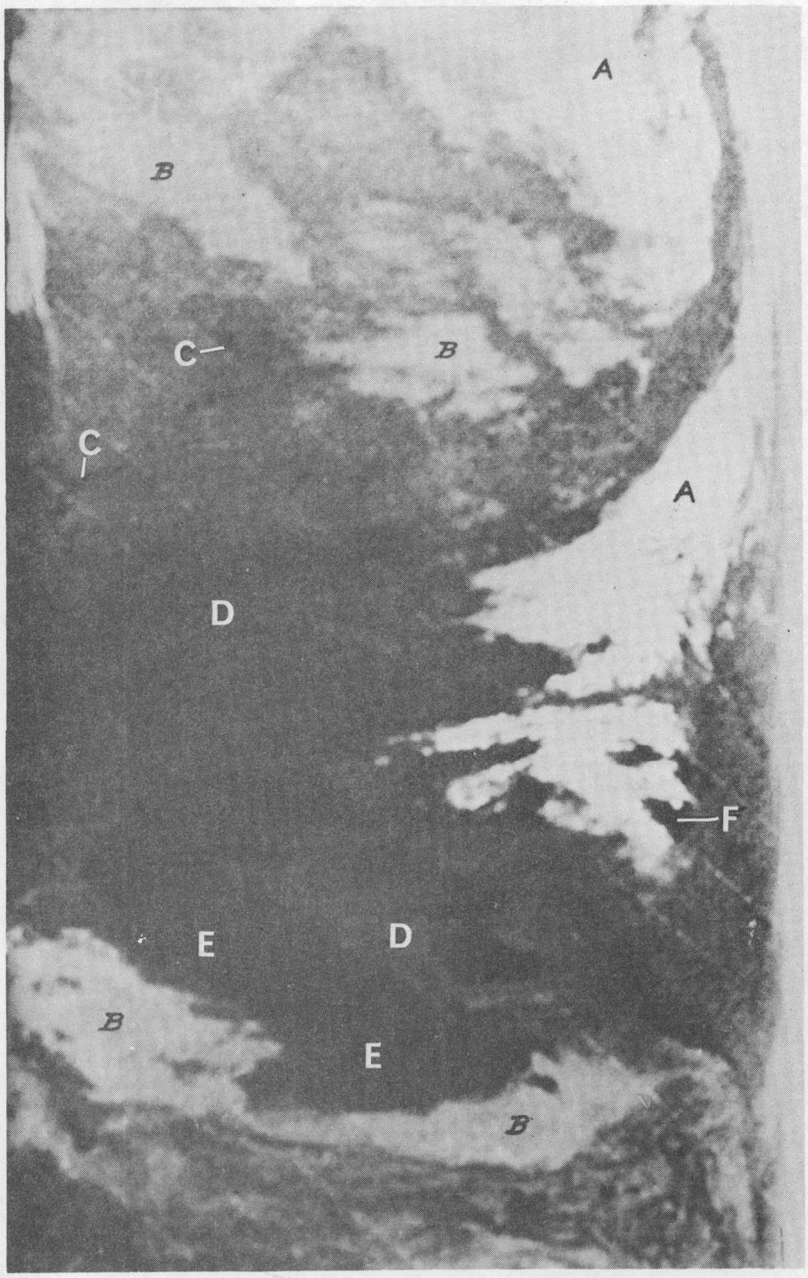

Figure 1 Nimbus I HRIR image of Caspian Sea region (magnified); A - high clouds, B - low clouds, C - Volga River, D - Caspian lowlands, E - Caspian Sea, F - Aral Sea. Orbit 037, Data Block 13.

Figure 2 Nimbus I HRIR image of southeast Africa (magnified); A - southern highlands of Tanganyika, B - Zanzibar, C - Tanganyika coastal lowlands, D - Lake Nyasa, E - Lake Chilwa, F - Nyasaland ranges, G - Zambesi Valley, H - southeast Rhodesian ranges, J - Basutoland ranges, K - Madagascar, L - Indian Ocean, X - low clouds, Y - high clouds. Orbit 037, Data Block 13.

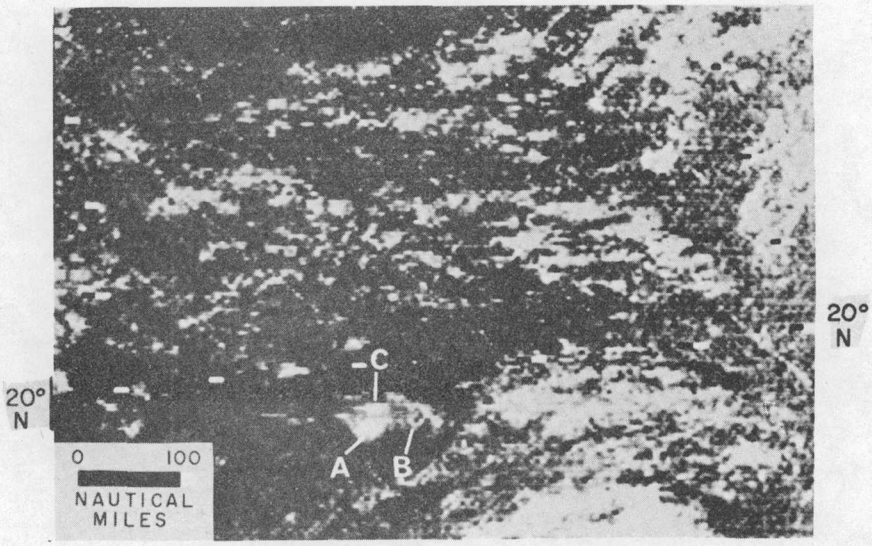

Figure 3 Nimbus I HRIR image of Hawaiian Islands and vicinity (magnified); A - Mauna Loa, B - Kilauea, C - Mauna Kea. Orbit 250, Data Block 191.

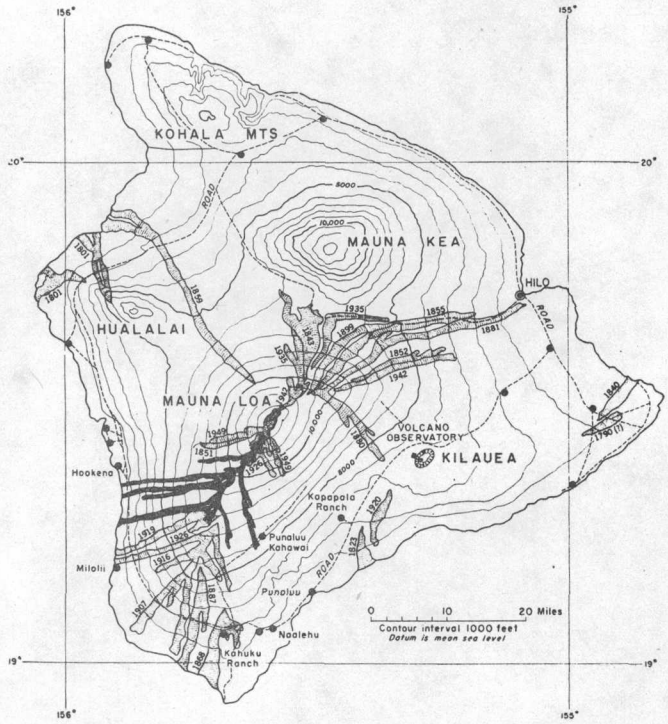

Figure 4. Relief Map of Hawaii

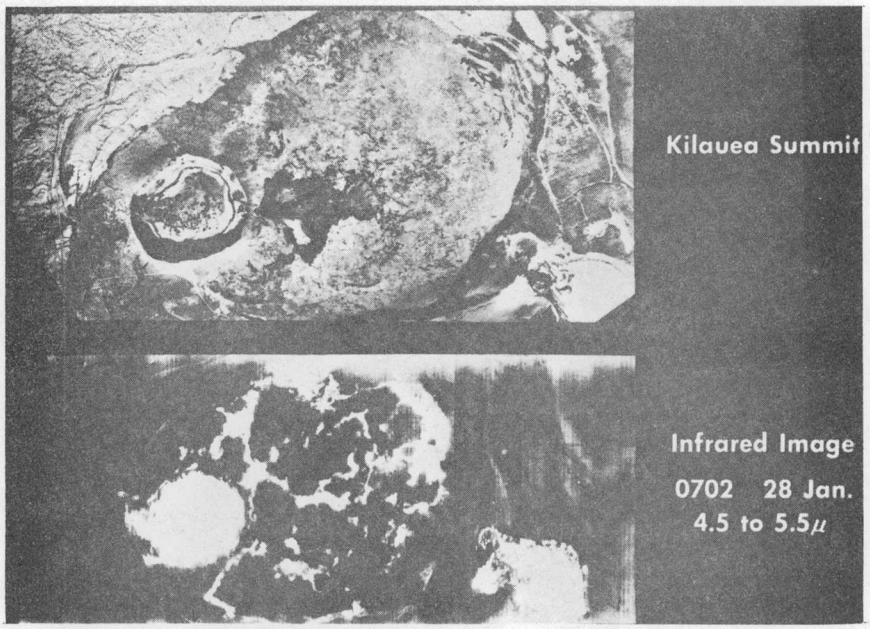

Figure 5 Low-altitude aerial infrared imagery and conventional photography of Kilauea Volcano, Hawaii.

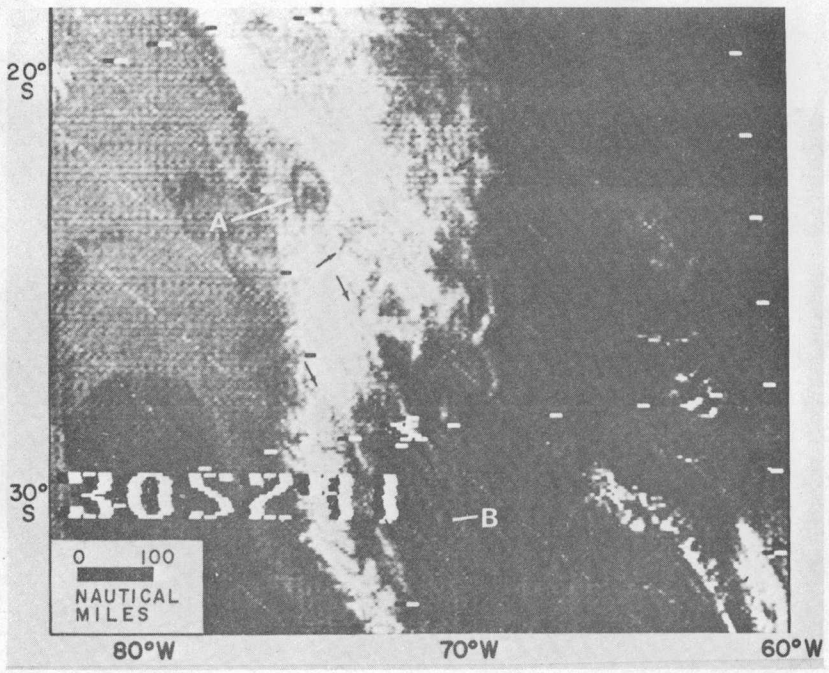

Figure 6 Nimbus I HRIR image of western South America (magnified); A - Atacama Desert, B - Sierra del Pie de Palo. Orbit 246, Data Block 184.

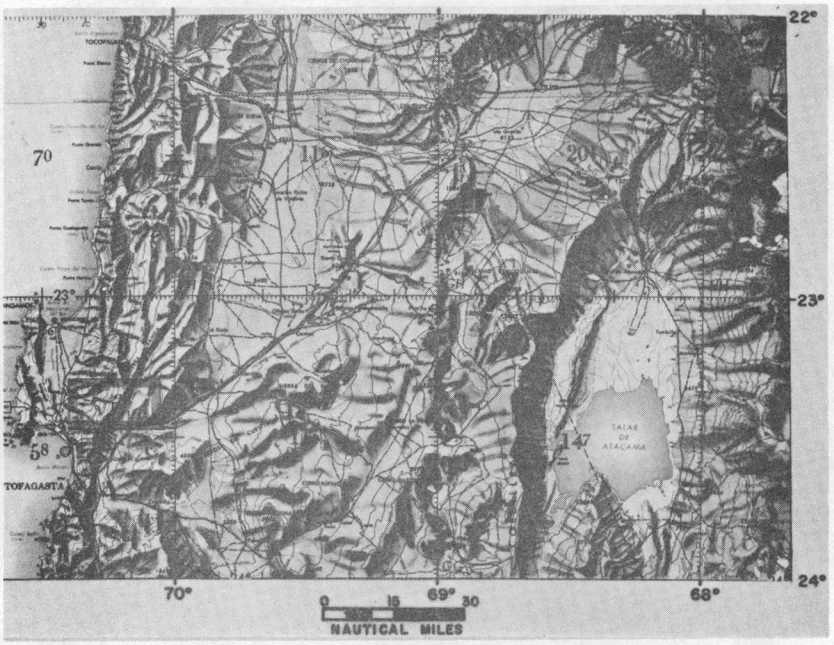

Figure 7 Relief map of Atacama Desert and Vicinity, Chile.

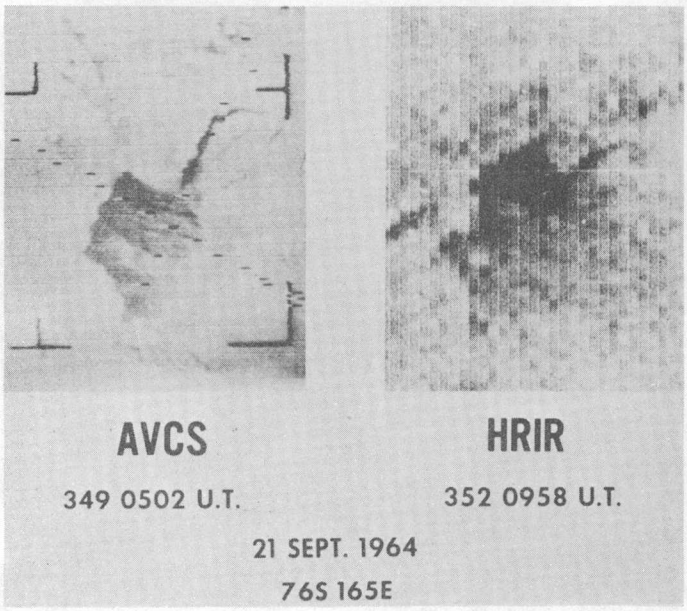

Figure 8 Nimbus I HRIR imagery and AVCS imagery, Ross Sea, Antarctica (magnified); Orbit 352, Data Block 317; Orbit 349.